

CRAB CAVITY AND CRYOMODULE DEVELOPMENT FOR HL-LHC*

F. Carra^{#1}, A. Amorim Carvalho¹, K. Artoos¹, S. Atieh¹, I. Aviles Santillana^{1,2},
 S. Belomestnykh^{3,4}, A. Boucherie¹, J.P. Brachet¹, K. Brodzinski¹, G. Burt⁵, R. Calaga¹,
 O. Capatina¹, T. Capelli¹, L. Dassa¹, S. U. De Silva⁶, J. Delayen⁶, T. Dijoud¹, H. M. Durand¹,
 G. Favre¹, P. Freijedo Menendez¹, M. Garlaschè¹, M. Guinchard¹, T. Jones^{5,7}, N.Kuder¹,
 S. Langeslag¹, R. Leuxe¹, Z. Li⁸, A. Macpherson¹, K. Marinov⁷, L. Marques Antunes Ferreira¹,
 P. Minginette¹, E. Montesinos¹, F. Motschmann¹, T. Nicol⁹, R. Olave⁶, C. Parente¹, H. Park⁶,
 S. Pattalwar⁷, L. Prever-Loiri¹, D. Pognat¹, A. Ratti¹⁰, E. Rigutto¹, V. Rude¹, M. Sosin¹,
 N. Templeton⁷, G. Vandoni¹, S. Verdú-Andrés³, G. Villiger¹, Q. Wu³, B. P. Xiao³, C. Zanoni¹

¹CERN, Geneva, Switzerland

²University Carlos III, 28911 Madrid, Spain

³BNL, Upton, NY 11973, USA

⁴Stony Brook University, Stony Brook, NY 11794, USA

⁵Cockroft Institute, Lancaster University, UK

⁶Old Dominion University, Norfolk, VA, 23529, USA

⁷STFC / Daresbury Laboratory, Daresbury, UK

⁸SLAC, Menlo Park, CA 94025, USA

⁹Fermilab, Batavia, IL 60510, USA

¹⁰LBNL, Berkeley, CA 94707, USA

Abstract

The HL-LHC project aims at increasing the LHC luminosity by a factor of 10 beyond the design value. The installation of a set of RF crab cavities is one of the key upgrades in the frame of this program: two concepts (Double Quarter Wave – DQW – and RF Dipole – RFD) have been proposed and are being designed in parallel in view of tests in the SPS before aiming at the final design for LHC.

This paper overviews the main design choices for the cryomodule and its different components, which have the goal of optimizing the structural, thermal and electromagnetic behaviour of the system, while respecting the existing constraints in terms of integration in the accelerator environment. Prototyping and testing of the most critical components, fabrication, preparation and installation strategies are also described.

INTRODUCTION

The LHC uses a 60 m common focusing channel on each side of the interaction region (IR), where the two counter-rotating beams have to be separated transversely to avoid parasitic collisions. The separation is performed by introducing a crossing angle at the interaction point

(IP), which increases with the inverse proportionality of the transverse beam size at the collision point. The non-zero crossing angle implies an inefficient overlap of the colliding bunches, thus reducing the luminosity. To recover the loss, one of the key elements of the HL-LHC upgrade will be the adoption of a crab-crossing scheme, provided by a set of compact SRF crab cavities [1]. Prior to installation in the LHC, a prototype two-cavity cryomodule will be built and tested in the SPS in 2017. An overview of the project planning until installation in the LHC is provided in Table 1 [2].

Table 1: Overview of Crab Cavity Planning

2013-2014	Cavity Testing & Cryomodule Design
2015-2016	SPS Cryomodule Fabrication
2017-2018	SPS Tests & LHC Pre-Series Module
2019-2024	LHC Cryomodule Construction & Testing
2024-2025	LHC Installation

The design and development of the cryomodule components is at an advanced stage [3]; the main sub-assemblies are summarized in Fig. 1 and described in the following paragraphs.

*The research leading to these results has received funding from the European Commission under the FP7 project HiLumi LHC, GA no. 284404, co-funded by the DoE, USA and KEK, Japan

#federico.carra@cern.ch

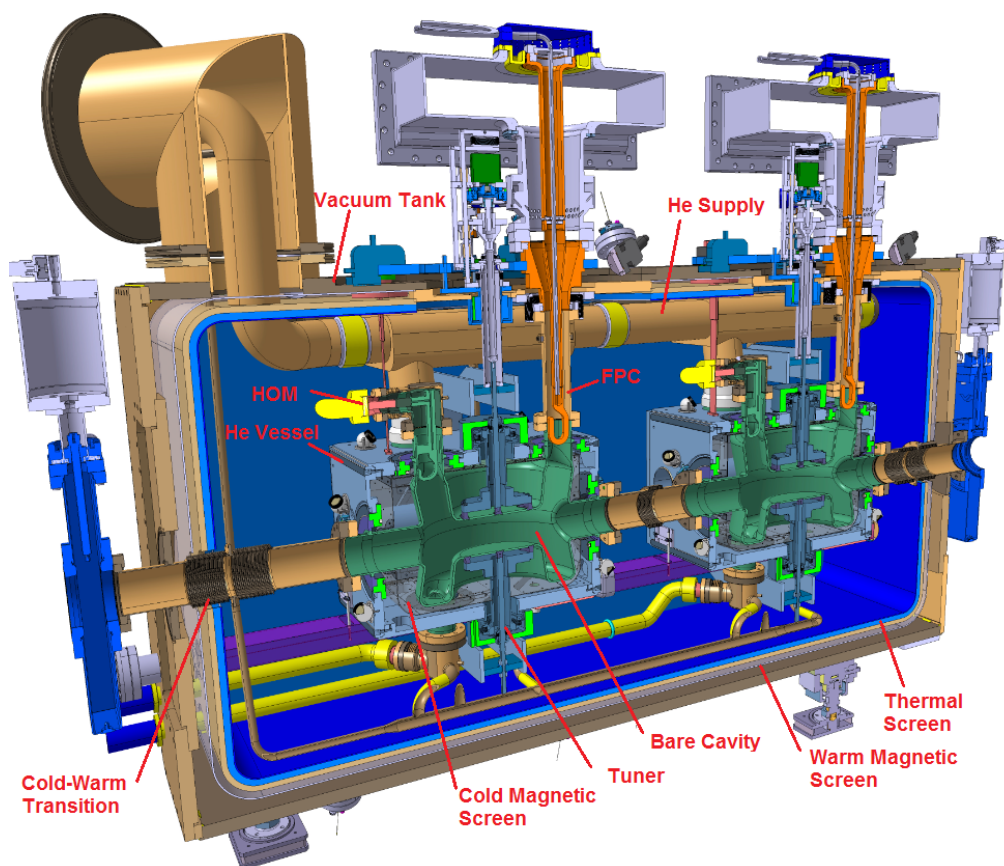


Figure 1: DQW cryomodule. A similar concept is being conceived for RFD.

DRESSED CAVITY

The assembly of the bare cavity with couplers and of the systems required around it in order to provide stiffness, cryogenic temperature, tuning and shielding from magnetic field is called dressed cavity.

The cavity is made of bulk niobium; its BCS resistance depends on operating temperature and frequency. At 4.5 K and 400 MHz such resistance is about 50 nΩ, more than 10 times larger than the value at 2 K. The complex shapes of the cavities may also be susceptible to microphonics caused by helium boil-off, hence operation below the lambda point of He is preferred. Furthermore, at 2 K the temperature margin before a quench is higher: this gives an additional margin for machine protection in case of a failure. For these reasons, operation at 2 K is the baseline.

Bare Cavity

Space limitations in the LHC led to the choice of unconventional shapes for the crab cavities. The three solutions proposed by the international collaboration are at least four times smaller in the crossing plane when compared to an equivalent elliptical cavity [4]. A prototype of each cavity was fabricated in 2012-13 and its performance validated at or beyond the nominal kick voltage of 3.4 MV [5][6][7]. Following the recommendation of a technical review held in May 2014 [8], only two cavity designs are now considered for the engineering development towards the SPS tests: the

Double Quarter Wave (DQW) and the RF Dipole (RFD), shown in Fig. 2.

The design of the cavity copes with several mechanical constraints: ensure elastic deformation under maximum pressure as well as during transport and handling; maximise tuning range; minimise sensitivity to pressure fluctuation; avoid buckling due to external pressure; maximise the frequency of the first mechanical natural mode. The cavity is made of 4mm-thick, electron-beam welded niobium sheets, and is cooled with saturated superfluid helium at 2 K. Each cavity is equipped with a helium tank, a tuning system, a fundamental RF power coupler (FPC), a field probe and two (RFD) or three (DQW) high-order mode couplers (HOM).

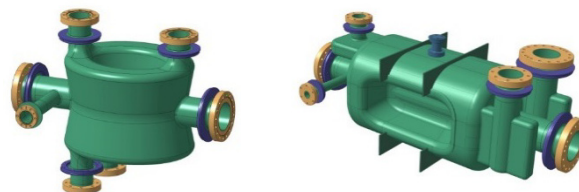


Figure 2: Cavity and interfaces. DQW, left; RFD, right.

Tuning System

The HL-LHC crab cavities shall operate at a frequency of 400.79 MHz, with a required resolution lower than 0.5 kHz in order to minimize the RF power needed to run the cavities. Several aspects contribute in changing the cavity geometry, and thus its frequency: manufacturing

shape errors, deformations induced by welding and assembling phases, surface treatments, thermal contractions from room temperature to 2 K and Lorentz detuning (estimated in the 1 kHz range). A tuning system with a range as large as possible is therefore required to mechanically correct the geometry variation, adjusting the frequency to the required value during operation. On top of this, the system shall induce a frequency sufficiently far from 400 MHz when the crab crossing is not required but the beam is present.

To maximise the reliability and maintainability of the tuning system, all moving and frictional components of the motorisation are placed outside of the cryostat, at room temperature: this also helps in minimising the damage induced by radiation to the sensitive components [9].

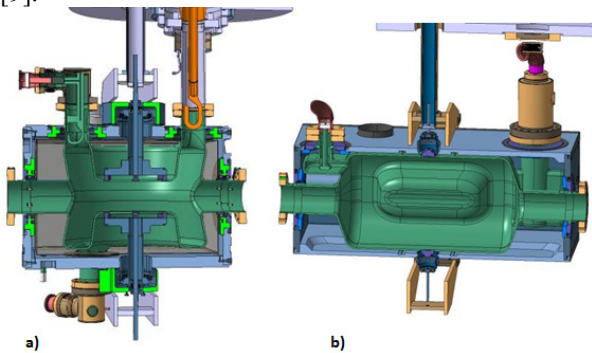


Figure 3: Tuning principle for DQW (a) and RFD (b).

For both DQW and RFD the tuning principle is the symmetrical vertical displacement between the two capacitive plates of the cavity (Fig. 3). In the first case, the tuning sensitivity is 186 kHz/mm and in the second, 345 kHz/mm. The motorisation induces a relative motion between two thin-walled coaxial tubes. The inner tube is connected, through a bellow on the helium vessel, to the top part of the cavity; the outer one is linked to a titanium frame also connected to the dressed cavity. A relative displacement between the two tubes will hence create a symmetric deformation of the cavity.

With a finite elements analysis, the tuning range estimated for the DQW cavity is ± 0.31 MHz for a displacement of 1.7 mm between the plates, while in the RFD case the range is ± 0.98 MHz for a displacement of 2.8 mm [9]. The tuning range for DQW is significantly lower: for this reason, a coarse pre-tuning system is also included in the design (Fig. 4).

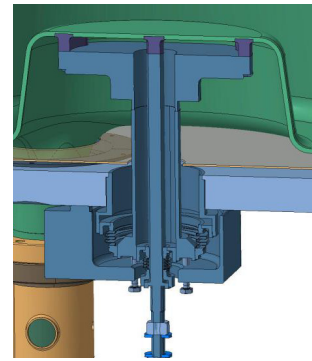


Figure 4: DQW pre-tuning: the deformation is imposed with screws at room temperature, after assembling the dressed cavity. Frequency sensitivity ~ 0.8 MHz/mm.

Helium Vessel

The helium tank is made of titanium grade 2, which has a thermal contraction coefficient very close to that of niobium (1.5 mm/m from 300 K to 2 K). The vessel was designed with the goal of minimising the stress acting on the cavity, to which it is rigidly connected, under the actions of the external loads. In particular, during cool-down, the cavity is subject to a He pressure of 1.8 bar and, in the DQW, to the force provided by the pre-tuning system.

The initial design was based on a fully-welded helium vessel, but it was discarded because of the high deformations that would have occurred after welding: dedicated tests showed that a 3 mm weld seam induces a deformation of 1 mm at the interface with the cavity (Fig. 5).

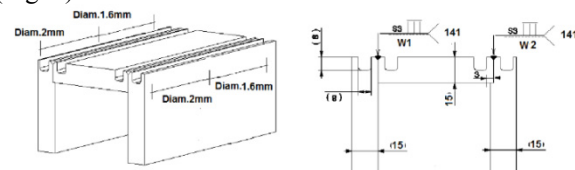


Figure 5: Test structure for evaluating the deformations after welding.

The new concept [10] is based on a bolted vessel (Fig. 6), with welds ensuring the vacuum-tightness with a minor structural role. The solution is unconventional; in the design analyses, the calculations were performed for the worst-case scenario, assuming no friction between the tank plates and all the load carried by the bolted joints and welds. The screws characteristics and tightening torque have been defined through a finite elements analysis of the assembly with ANSYS, evaluating the reaction forces and moments at each contact [11].

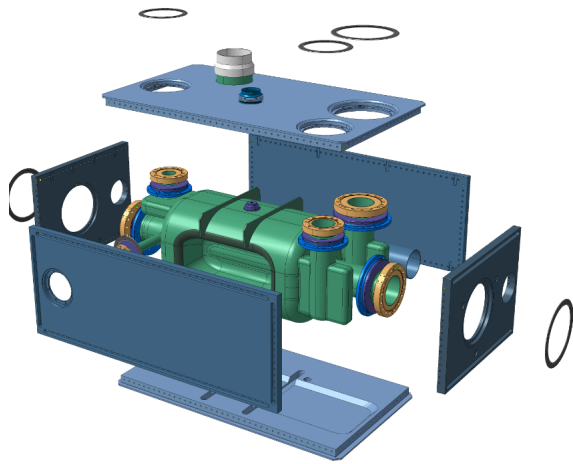


Figure 6: Assembling of the bolted He vessel (RFD).

The material chosen for the screws is titanium grade 5, because of its high proof stress and the same coefficient of thermal expansion of the vessel plates. FEA analyses of the He tank showed satisfactory results: the maximum allowable stress for the component is 275 MPa, to be compared with the calculated equivalent stress depicted in Fig. 7.

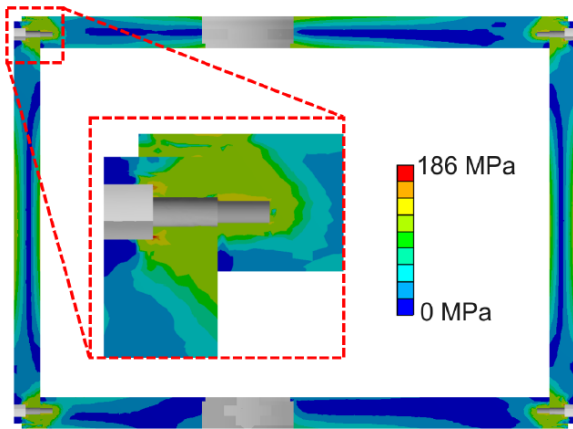


Figure 7: Stress through a plane in the middle of the tank. Peak stresses around the bolt head are an effect of numerical errors.

The resistance of the cavity, rigidly connected to the He vessel, has been verified according to the EN13445-3 Standards [12]. In some areas, the equivalent stress is higher than the allowable stress of Nb, which is 50 MPa (Fig. 8). This requires a more detailed evaluation of the stress nature, according to the “Design by Analysis – method based on stress categories” contained in the Standards. For each relevant point, membrane (P_m), bending (P_b), primary (P) and secondary (Q) stresses have been calculated. The primary stress is generated by gravity and pressure, while the pre-tuner induces secondary stresses, which are self-limiting. With reference to Fig. 8, a detailed analysis of the most loaded areas is shown in Table 2.



Figure 8: Equivalent stress on cavities - DQW (top) and RFD (bottom).

Table 2: Stress Assessment for most Loaded Areas

Zone	Stress category	Allowable stress		Calculated stress
			[MPa]	
1	P_m	f	50	27
	$P_m + P_b$	$1.5f$	75	55
	$\Delta(P+Q)$	$3f$	150	110
2	P_m	f	50	7
	$P_m + P_b$	$1.5f$	75	58
	$\Delta(P+Q)$	$3f$	150	121
3	P_m	f	50	29
	$\Delta(P+Q)$	$3f$	150	86

SUPPORTING SYSTEM

Before operation, the orientation and position of the cavity is adjusted by means of a plate rigidly connected to the cavity itself. The connection is done through the FPC coupler and a set of additional supports; the plate is isotatically supported in three points, whose position can be adjusted to move and align the cavity (Fig. 9).

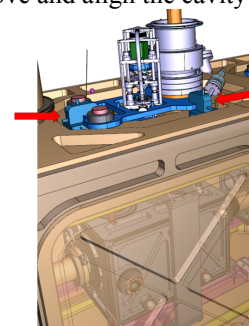


Figure 9: positioning plate (in blue) and supports (highlighted by red arrows).

Several design solutions for the supporting system were analysed: at a first stage, to minimise the heat transfer

from the external ambient to the cold mass, the design foresaw thin supports complemented by an intercavity connection. This solution was discarded because of the insufficient stiffness and the difficulties expected in the alignment phase. The final solution, with blade supports, guarantees a higher stiffness: the main concepts are shown in Fig. 10.

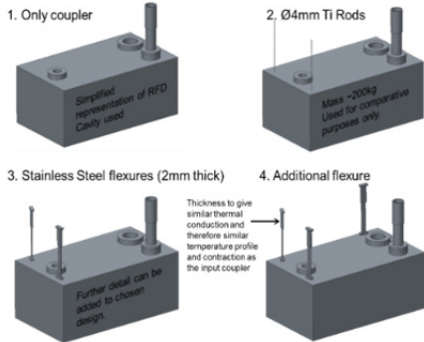


Figure 10: Support options considered for SPS Compact Crab Cavities.

The structural and modal response of the different solutions was compared with finite elements analyses. The results (Table 3) show that the performance of the supporting system is significantly increased with a ‘blade’ type flexure arrangement [13]. These give an increase in overall stiffness whilst still allowing for thermal contraction on cool down to 2 K towards the fixed point, which is the input coupler.

Table 3: Structural and Model Response of the Solutions Analysed

Solution	Def. Max. [mm]	Mode 1 [Hz]	Mode 2 [Hz]	Mode 3 [Hz]	Mode 4 [Hz]
1	3.9	7.7	8.3	16.1	61.1
2	0.24	8.5	25.3	38.3	70.9
3	0.025	25.1	48.3	56.5	122
4	0.01	27.2	50.15	66.9	174

MAGNETIC SHIELDING

The magnetic shielding of the cold mass is provided by a warm outer screen and one cold inner screen per cavity. This solution limits the magnetic field on the cavity surface to less than 1 μ T, as per specification [14].

The outer shield is made of 3 mm thick mu-metal sheets: Fig. 11 shows the magnetic field amplitude for an applied external field of 200 μ T in the beam axis direction, which is the expected value during operation in the SPS [15].

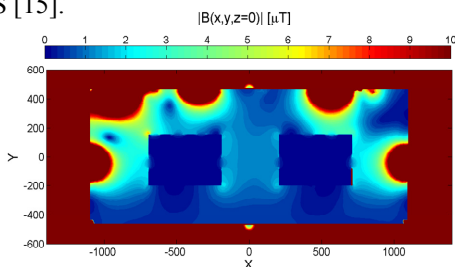


Figure 11: Magnetic field amplitude with inner and outer magnetic shields.

The addition of internal shields is due to the presence of large apertures in the warm screen, which allow the passage of couplers, survey instrumentation and beam pipes. The cold shields are immersed in the He bath. They consist in 1 mm thick plates in the Ni-Fe-Mo alloy Aperam Cryophy® [16], which decreases the magnetic field on the cavities down to the nT range, as shown in Fig. 12.

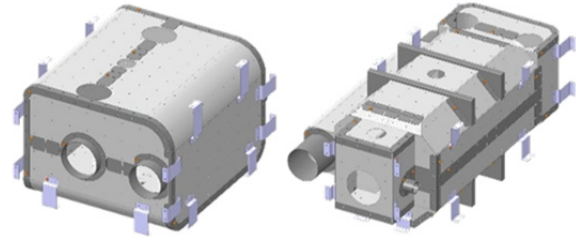


Figure 12: Magnetic cold screen: DQW (left) and RFD (right).

THERMAL SHIELDING

The thermal screen (Fig. 13) is in aluminium alloy, covered with Multi-Layer Insulation sheets (MLI) in order to minimize the radiative heat exchange between the cold mass and the surroundings at 300 K [17]. It is thermalized at with He gas; with this configuration, the heat exchange is lower than 1 W.

For hosting the instrumentation necessary for the alignment measurements, holes are machined in the thermal screen: this increases the heat losses to the cold mass, because of the high equivalent emissivity of the hole surface. The total heat losses through radiation are included in Table 4.

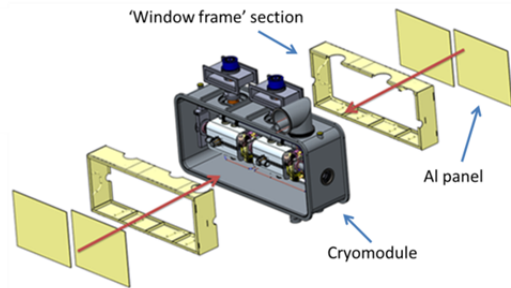


Figure 13: Thermal shielding assembly.

HIGH-ORDER MODES COUPLERS

High-order modes (HOM) couplers are needed to damp the detrimental modes with frequency higher than the fundamental one, minimising the power dissipation and beam instability that would come from such modes. Three HOM are embedded in each DQW cavity, while two are present in the RFD solution [18]. The HOM antenna has a hook shape and is made of superconductive Nb, to minimise the power absorption of the component, thus limiting its temperature increase (Fig. 14). In the preliminary design phase, copper was also considered for the HOM hook, but an iterative HFSS/ANSYS analysis showed that the temperature induced by the RF losses would be well above the melting point of the metal.

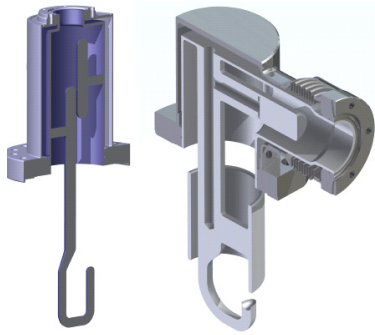


Figure 14: HOM: RFD (left) and DQW (right).

The pre-series of DQW HOM is currently under fabrication at CERN (see Fig. 15), and the RFD component machining is also planned to follow shortly.



Figure 15: First prototype of the DQW HOM hook built at CERN.

FUNDAMENTAL POWER COUPLER

The Fundamental Power Coupler (FPC) is composed of a stainless steel tube and an inner Cu OFE hook (Fig. 16). The stainless steel tube is thermalized at 80 K in the most favourable position, to minimize the required refrigerating power and limit the losses to the 2 K bath.

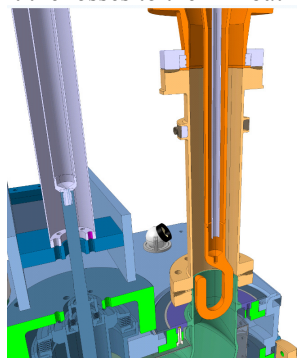


Figure 16: Section view of the FPC hook.

The shape and penetration of the hook was optimized via iterative analysis HFSS/ANSYS, in order to minimise the dissipated power for a required RF coupling and, consequently, the maximum copper temperature. A too high temperature on the component could induce creep deformations and a high radiation flux on the cold mass. For this reason, a cooling channel, with circulating water,

is included in the core of the hook straight section. The maximum FPC hook temperature expected in operation is about 100 °C for a total loss on the component equal to ~100 W (Fig. 17).

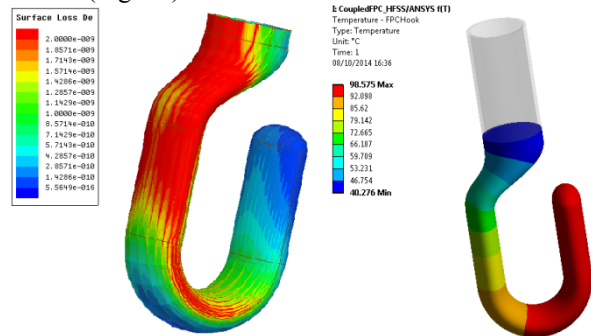


Figure 17: Left: surface loss density, calculated with HFSS and scaled to an electric field of 1 V/m. Right: temperature increase on FPC hook in operation.

VACUUM VESSEL

The most external layer of the cryomodule is the vacuum vessel. The cold mass is kept under insulation vacuum to eliminate the thermal losses which would otherwise be induced through convection and gas conduction. The maximum dimensions of the envelope composed by the vacuum tank and ancillary components are:

- Length: 2900 mm for the RFD, 2750 mm for the DQW
- Width: 1050 mm
- Height: 2350 mm (1400 mm above the beam, 950 mm below)

The vacuum vessel is currently in the design phase; 15 mm thick stainless steel plates are the baseline for the component. Reinforcing ribs are foreseen to improve the wall stiffness, to minimise the deformation without increasing excessively the total weight. The rib thickness is 50 mm; results of the preliminary finite elements analysis are shown in Fig. 18.

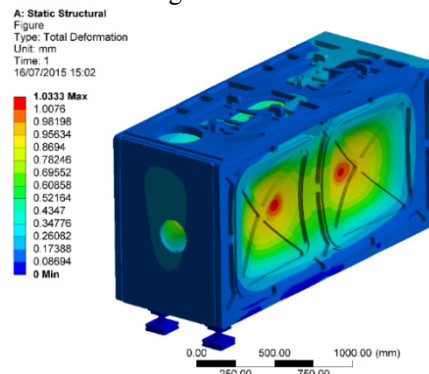


Figure 18: Total deformation of the vacuum vessel under the action of the external pressure.

HEAT LOADS SUMMARY

In order to evaluate the required cryogenic power for the assembly, a balance of the heat losses to the 2 K and

80 K lines has been performed and is reported in Table 4. The breakdown is done between two types of losses: the static losses occur mainly because of conduction through the interfaces between cavity and external ambient and through radiation. The dynamic losses, on the other hand, are additionally generated when the RF power is on and the beam is circulating, and are due to Joule effect and beam energy deposition.

Table 4: Heat Loads Balance

	DQW		RFD	
	2K	80K	2K	80K
Static				
Radiation	3	35	3	35
CWT	0.2	2	0.2	2
Supports	0.8	30	0.8	30
FPC	4	100	4	100
Instrumentation	1	0	1	0
HOM/Pickup	2.5	10	1.7	10
Tuner	0.3	10	0.3	10
Total static	11.8	187	11	187
Dynamic				
Cavity	6	0	6	0
FPC	5.6	10	5.6	20
HOM/Pickup	7.2	120	5.5	80
Beam	0.5	0	0.5	0
Total Dynamic	19.3	130	17.6	100
TOTAL	31.1	317	28.6	287

CONCLUSIONS

RF crab cavities are one of the key upgrades in the frame of the HL-LHC project, which aims at increasing the LHC luminosity by a factor of 10.

The behaviour of the two different concepts (DQW and RFD) will be tested in the SPS in 2017. The engineering design of the dedicate cryomodules is at an advanced stage and material procurement, prototyping and testing of the most critical components has been launched by CERN and the international project partners. Other important aspects such as thermal and magnetic systems, supporting, alignment, tuning are also being assessed, fully in line with the project schedule.

REFERENCES

[1] High Luminosity Large Hadron Collider (HL-LHC), website: <http://hilumilhc.web.cern.ch>

- [2] R. Calaga, A. Ratti, "Update on cavity production and planning", presented at the 4th HiLumi Meeting, KEK, 2014.
- [3] S. Patalwar et al., "Conceptual design of a cryomodule for compact crab cavities for Hi-Lumi LHC", MOP087, SRF2013, Paris, 2013.
- [4] S. Verdu-Andres et al., "Crab Cavities for Colliders: Past, Present and Future", Proceedings of ICHEP 2014, Valencia (2014).
- [5] S. U. De Silva and J. R. Delayen, "Cryogenic test of a proof-of-principle superconducting rf-dipole deflecting and crabbing cavity", Phys. Rev. ST Accel. Beams 16, 082001 (2013).
- [6] B. Hall *et al.*, "Testing and Dressed Cavity Design for the HL-LHC 4R Crab Cavity", WEPRI048, IPAC'14, Dresden, Germany (2014).
- [7] B. Xiao *et al.*, "Design, prototyping, and testing of a compact superconducting double quarter wave crab cavity", Phys. Rev. ST Accel. Beams 18, 041004, 2015.
- [8] A. Yamamoto *et al.*, Crab cavity system external review report, CERN-ACC-2014-0093, 2014.
- [9] K. Artoos *et al.*, "Development of SRF Cavity Tuners for CERN", these proceedings, THPB060, SRF2015, Whistler, BC, Canada, 2015.
- [10] C. Zanoni *et al.*, "Design of Dressed Crab Cavities for the HL-LHC Upgrade", these proceedings, THPB070, SRF2015, Whistler, BC, Canada, 2015.
- [11] VV.AA., "VDI2230 – Systematic calculation of highly-stressed bolted joints", December 2014.
- [12] VV.AA., "EN13445-3 – Unfired pressure vessels", 2008.
- [13] T. Jones, "Dressed cavity support options", CERN Indico, <https://indico.cern.ch/event/405409/>, 2015.
- [14] P. Baudrenghien *et al.*, "Functional specification of the LHC prototype crab cavity system", CERN-ACC-Note-2013-003, 2013.
- [15] J. Bauche, A. Macpherson, "Estimate of Ambient Magnetic Field in the SPS Crab Cavity Location", CERN, 2014.
- [16] M. Masizawa *et al.*, "Magnetic shielding: our experience with various shielding materials", Proceedings of SRF 2013, Paris, 808, (2013).
- [17] N. Templeton *et al.*, "Design of the Thermal and magnetic Shielding for the LHC High Luminosity Crab Cavity Upgrade", these proceedings, THPB101, SRF2015, Whistler, BC, Canada, 2015.
- [18] C. Zanoni *et al.*, "Engineering Design and Prototype Fabrication of HOM Couplers for HL-LHC Crab Cavities", these proceedings, THPB069, SRF2015, Whistler, BC, Canada, 2015.